Latin American Journal of Solids and Structures
www.lajss.org

Elastic analysis of pressurized thick FGM cylinders with exponential variation of material properties using TSDT

Abstract

In this research, the general governing set of differential equations for axisymmetric thick FG pressurized cylinders with exponential function of material properties is derived based on third order shear deformation theory. Afterwards, a general analytical solution of governing equations based on Eigen values problems is conducted for cylinders under clamped ends condition. Furthermore, a numerical modeling is done in order to compare the results of two different solution and prove the accuracy of analysis. The displacements and stresses resulted from FEM and TSDT are depicted for a case study along the radial and longitudinal direction of the cylinder. Afterwards, the effect of internal and external pressure, FGM inhomogeneity constants and higher order approximation is investigated. The results of SDT and FEM show good agreement and prove the fact that usage of FGM cylinders causes lower values of displacements and stresses.

Keywords

Exponential function; FGM; thick cylinder; TSDT; FEM.

M. Ghannad
H. Gharooni*

Faculty of Mechanical Engineering,
Shahrood University, Shahrood, Iran

Corresponding author:
*gharooni.hamed@gmail.com

http://dx.doi.org/10.1590/1679-78251491

Received 31.07.2014
In revised form 23.03.2015
Accepted 25.03.2015
Available online 10.04.2015

1 INTRODUCTION

Axisymmetric hollow cylindrical shells are common structural elements in many engineering applications, including pressure vessels, submarine hulls, ship hulls, wings and fuselages of airplanes, containment structures of nuclear power plants, pipes, exteriors of rockets, missiles, automobile tires, concrete roofs, chimneys, cooling towers, liquid storage tanks, and many other structures. In order to optimize the weight, mechanical strength, displacement and stress distribution of a shell, one approach is to use shells with functionally graded materials. FGMs or heterogeneous materials are advanced composite materials with microscopically inhomogeneous characters.

The first order shear deformation theory (FSDT) for homogeneous thick cylindrical shells was expressed by Mirsky and Hermann (1958). Reddy and Liu (1985) developed a simple higher order shear deformation shell theory, in which the transverse shear strains are assumed to be parabolically distributed across the shell thickness and which contains the same number of dependent unknowns

as in the first-order shear deformation theory, and no shear correction factors are required. Greenspon (1960) compared the results of different theories of thick-walled cylindrical shells. Fukui and Yamanaka (1992) used the Navier solution for derivation of the governing equation of a thick-walled FGM tube under internal pressure and solved the obtained equation numerically by means of the Runge-Kutta method. Simkins (1994) used the FSDT for determining displacement in a long and thick tube subjected to moving loads. Eipakchi et al. (2003) have investigated the governing equations of homogeneous cylinders with variable thickness using FSDT and represent the solution of the equations using perturbation theory. Eipakchi et al. (2008) further extended their previous work by considering homogenous and isotropic conical shells with variable thickness using FSDT and SSDT (second-order shear deformation theory) and solved the conducted equations by perturbation theory.

Hongjun et al. (2006) indicated the exact solution of FGM hollow cylinders in the state of plane strain with exponential function of elasticity modulus along the radius. Zhifei et al. (2007) analyzed heterogeneous cylindrical shells with power function of elasticity modulus by the usage of multilayer method with homogeneous layers. Thick-walled FGM cylinders in plane strain state with exponentially-varying material properties were solved by Tutuncu (2007) using Frobenius method. Tutuncu and Temel (2009) determined axisymmetric displacements and stresses in functionally graded hollow cylinders, disks and spheres subjected to uniform internal pressure by the usage of plane elasticity theory and complementary functions method. Zamani Nejad et al. (2009) developed 3-D set of field equations of FGM thick shells of revolution in curvilinear coordinate system by tensor calculus. Ghannad and Zamani Nejad (2010) presented the general method of derivation and the analysis of internally pressurized thick-walled cylinders with clamped-clamped ends. Eipakchi (2010) calculated stresses and displacements of a thick conical shell with varying thickness under nonuniform internal pressure analytically using third-order shear deformation theory (TSDT). Ghannad and Zamani Nejad (2012) presented a complete elastic solution of pressurized thick cylindrical shells made of heterogeneous functionally graded materials by the usage of plane elasticity theory. Kumar et al. (2013) investigated static analysis of skew composite shells by developing a finite element (FE) model based on higher order shear deformation theory (HSDT). They assumed a realistic parabolic variation of transverse shear strains through the shell thickness and considered Sander's approximations to include the effect of three curvature terms in the strain components of composite shells. Ghannad et al. (2013) presented a closed form analytical solution for clamped-clamped thick cylindrical shells with variable thickness made of functionally graded materials subjected to constant internal pressure based on FSDT.

Considering the literature review prove the lack of exact or accurate analytical solution for thick FGM cylinders with an exponential variation of material properties. In order to consider the effect of shear stresses and strains, shear deformation theory is used for analytical solution of axisymmetric thick FG pressurized cylinders under clamped ends condition in this paper. The governing set of differential equations for an axisymmetric pressurized cylinder have been derived based on third-order shear deformation theory and a general solution is conducted for clamped boundary conditions. The material properties of FG cylinder are assumed to be heterogeneous with radially varying elastic modulus continuously along the thickness with an exponential function and constant Poisson's ratio. The results of SDT are compared with the results of a numerical modeling for pressurized FG cylinder based on FEM. Beside the investigation of internal and external pressure effect,

the higher order approximation is compared with lower one and improvement of the results by the usage of higher order approximation has been shown.

2 BASIC FORMULATION

Considering the rotation of the elements in the cross section of a cylinder, the shear strain is not zero. Taking into account shear stresses and strains, deformation at every layer of the cylinder could be simulated by the usage of shear deformation theory based on principal work. Therefore, the displacement field could be assumed as a polynomial of a variable (z) through the thickness of cylinder. As the number of terms in the polynomial function increase, the approximate solution will be improved. Writing the radius of every layer in terms of radius of mid-plane R and distance of every layer with respect to mid-plane z, we have (Figure 1):

$$r = R + z \tag{1}$$

x and z are the length and the thickness variables. The parameters x and z have been changed in the following intervals:

$$0 \le x \le L \ , \ -\frac{h}{2} \le z \le +\frac{h}{2} \tag{2}$$

where h and L are the thickness and the length of the cylinder.

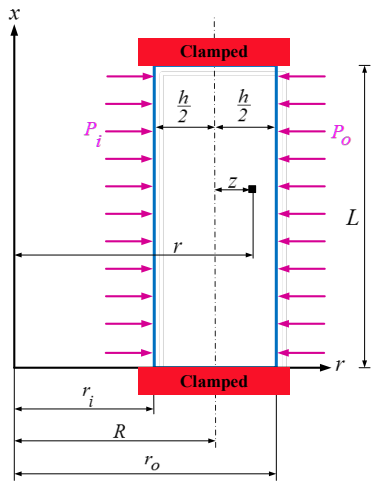

Figure 1: Geometry of the thick pressurized cylindrical shell.

Based on TSDT, the component of deformation can be stated by variables that includes the displacement and rotation. For an axisymmetric cylindrical shell, axial and radial components of displacement field are assumed to be in the following form (Eipakchi, 2010):

$$\begin{cases} U_x = u_0(x) + zu_1(x) + z^2u_2(x) + z^3u_3(x) \\ U_\theta = 0 \\ U_z = w_0(x) + zw_1(x) + z^2w_2(x) + z^3w_3(x) \end{cases} \tag{3}$$

$u_0(x)$ and $w_0(x)$ are the displacement components of the middle surface. Also, $u_1(x)$ and $w_1(x)$ are the rotations of the normal to the middle surface with respect to the x- and z- axes, respectively. u_0, u_1, u_2, u_3 and w_0, w_1, w_2, w_3 are the unknown functions of x used to determine the displacement field.

The mechanical kinematic relations in the cylindrical coordinates system for an axisymmetric cylinder are:

$$\begin{cases} \varepsilon_x = \dfrac{\partial U_x}{\partial x} = \dfrac{\mathrm{d}u_0}{\mathrm{d}x} + \dfrac{\mathrm{d}u_1}{\mathrm{d}x} z + \dfrac{\mathrm{d}u_2}{\mathrm{d}x} z^2 + \dfrac{\mathrm{d}u_3}{\mathrm{d}x} z^3 \\ \varepsilon_\theta = \dfrac{U_z}{r} = \dfrac{w_0 + w_1 z + w_2 z^2 + w_3 z^3}{R + z} \\ \varepsilon_z = \dfrac{\partial U_z}{\partial z} = w_1 + 2w_2 z + 3w_3 z^2 \\ \gamma_{xz} = \dfrac{\partial U_x}{\partial z} + \dfrac{\partial U_z}{\partial x} = \left(u_1 + \dfrac{\mathrm{d}w_0}{\mathrm{d}x}\right) + \left(2u_2 + \dfrac{\mathrm{d}w_1}{\mathrm{d}x}\right) z + \left(3u_3 + \dfrac{\mathrm{d}w_2}{\mathrm{d}x}\right) z^2 + \dfrac{\mathrm{d}w_3}{\mathrm{d}x} z^3 \end{cases} \tag{4}$$

Considering the dimensionless radial coordinate $(\overline{r})$ as the ratio of radial coordinate (r) upon internal radius (r_i):

$$\overline{r} = \frac{r}{r_i} \tag{5}$$

Modulus of elasticity E is supposed to be an exponential function of the dimensionless radial coordinate:

$$E(\overline{r}) = E_i e^{n(\overline{r}-1)} \tag{6}$$

Here E_i is the modulus of elasticity at the inner surface of the cylinder (r_i) and n is the inhomogeneity constant of FG material. The Poisson's ratio, ν, for a thick-walled cylindrical pressure vessel of FGM varies in a small range. Furthermore, its effects on mechanical stresses are insignificant. For simplicity, the Poisson's ratio is assumed to be constant.

On the basis of the constitutive equations for inhomogeneous and isotropic materials, the stress-strain relations are as follows:

$$\begin{cases} \begin{Bmatrix} \sigma_x \\ \sigma_\theta \\ \sigma_z \end{Bmatrix} = \begin{bmatrix} \lambda + 2\mu & \lambda & \lambda \\ \lambda & \lambda + 2\mu & \lambda \\ \lambda & \lambda & \lambda + 2\mu \end{bmatrix} \begin{Bmatrix} \varepsilon_x \\ \varepsilon_\theta \\ \varepsilon_z \end{Bmatrix} \\ \tau_{xz} = \mu \gamma_{xz} \end{cases} \tag{7}$$

where λ and μ are the Lame's constants. Considering variable elasticity modulus for the FGM materials, these two parameters are as follows:

$$\lambda = \frac{\nu E(z)}{\left(1+\nu\right)\left(1-2\nu\right)} \tag{8}$$

$$\mu = \frac{E(z)}{2\left(1+\nu\right)} \tag{9}$$

The distribution of elasticity modulus in Eq. (6) could be re-written as a function of z by substituting r from Eq. (1) into Eq. (5):

$$E(z) = E_i e^{n\left(\frac{R+z}{r_i}-1\right)} \tag{10}$$

The axial forces based on normal components of stress are as follows:

$$\begin{Bmatrix} N_x \\ N_\theta \\ N_z \end{Bmatrix} = \int_{-h/2}^{h/2} \begin{Bmatrix} \sigma_x \left(1+z/R\right) \\ \sigma_\theta \\ \sigma_z \left(1+z/R\right) \end{Bmatrix} \mathrm{d}z \tag{11}$$

The bending moments based on normal components of stress are as follows:

$$\begin{Bmatrix} M_x \\ M_\theta \\ M_z \end{Bmatrix} = \int_{-h/2}^{h/2} \begin{Bmatrix} \sigma_x \left(1+z/R\right) \\ \sigma_\theta \\ \sigma_z \left(1+z/R\right) \end{Bmatrix} z\,\mathrm{d}z \tag{12}$$

The higher-order bending moments based on normal components of stress are as follows:

$$\begin{Bmatrix} P_x \\ P_\theta \\ P_z \end{Bmatrix} = \int_{-h/2}^{h/2} \begin{Bmatrix} \sigma_x \left(1+z/R\right) \\ \sigma_\theta \\ \sigma_z \left(1+z/R\right) \end{Bmatrix} z^2\,\mathrm{d}z \tag{13}$$

$$\begin{Bmatrix} S_x \\ S_\theta \end{Bmatrix} = \int_{-h/2}^{h/2} \begin{Bmatrix} \sigma_x \left(1+z/R\right) \\ \sigma_\theta \end{Bmatrix} z^3\,\mathrm{d}z \tag{14}$$

The shear force based on shear stress is as follows:

$$Q_x = \int_{-h/2}^{h/2} \tau_{xz} \left(1+\frac{z}{R}\right) \mathrm{d}z \tag{15}$$

The torsional moment based on shear stress is as follows:

$$M_{xz} = \int_{-h/2}^{h/2} \tau_{xz} \left(1+\frac{z}{R}\right) z\,\mathrm{d}z \tag{16}$$

The higher-order torsional moments based on shear stress are as follows:

$$P_{xz} = \int_{-h/2}^{h/2} \tau_{xz} \left(1 + \frac{z}{R}\right) z^2 \, \mathrm{d}z \tag{17}$$

$$S_{xz} = \int_{-h/2}^{h/2} \tau_{xz} \left(1 + \frac{z}{R}\right) z^3 \, \mathrm{d}z \tag{18}$$

Based on the principle of virtual work, the variation of strain energy of the elastic body $\left(U\right)$ is equal to the variation of external work due to pressure $\left(W\right)$.

$$\delta U = \delta W \tag{19}$$

where U is the total strain energy of the elastic body and W is the total external work due to internal and/or external pressure. The strain energy is

$$\begin{cases} U = \iiint_V U^* \mathrm{d}V \ , \ \mathrm{d}V = r \, \mathrm{d}r \, \mathrm{d}\theta \, \mathrm{d}x = \left(R + z\right) \mathrm{d}x \, \mathrm{d}\theta \, \mathrm{d}z \\ U^* = \frac{1}{2} \left\{\varepsilon\right\}^T \left\{\sigma\right\} = \frac{1}{2} \left(\sigma_x \varepsilon_x + \sigma_\theta \varepsilon_\theta + \sigma_z \varepsilon_z + \tau_{xz} \gamma_{xz}\right) \end{cases} \tag{20}$$

and the external work is

$$\begin{cases} W = \iint_S \left(\vec{f}_{sf} \cdot \vec{u}\right) \mathrm{d}S \ , \ \mathrm{d}S = r \, \mathrm{d}\theta \, \mathrm{d}x \\ \left(\vec{f}_{sf} \cdot \vec{u}\right) \mathrm{d}S = \left(P_i r_i - P_o r_o\right) U_z \, \mathrm{d}\theta \, \mathrm{d}x \end{cases} \tag{21}$$

where $\vec{f}_{sf}$ is the surface force of the pressurized cylinder. Furthermore, P_i and P_o are the horizontal pressures in the internal and external surfaces. Variation of the strain energy can be expressed as follows:

$$\begin{cases} \delta U = R \int_0^{2\pi} \int_0^L \int_{-h/2}^{h/2} \delta U^* \left(1 + \frac{z}{R}\right) \mathrm{d}z \ \mathrm{d}x \ \mathrm{d}\theta \\ \Rightarrow \frac{\delta U}{2\pi} = R \int_0^L \int_{-h/2}^{h/2} \left(\sigma_x \delta\varepsilon_x + \sigma_\theta \delta\varepsilon_\theta + \sigma_z \delta\varepsilon_z + \tau_{xz} \delta\gamma_{xz}\right) \left(1 + \frac{z}{R}\right) \mathrm{d}z \ \mathrm{d}x \end{cases} \tag{22}$$

and the variation of the external work is

$$\begin{cases} \delta W = \int_0^{2\pi} \int_0^L \left[P_i r_i - P_o r_o\right] \delta U_z \mathrm{d}x \ \mathrm{d}\theta \\ \Rightarrow \frac{\delta W}{2\pi} = \int_0^L \left[P_i \left(R - \frac{h}{2}\right) - P_o \left(R + \frac{h}{2}\right)\right] \delta U_z \ \mathrm{d}x \end{cases} \tag{23}$$

Substituting Eqs. (4), (7) and (10) into Eqs. (22) and (23), using Eq. (19) and carrying out the integration by parts, the equilibrium equations for the cylindrical shell with constant thickness under internal and external pressure are obtained in the form of:

$$\begin{cases} R\dfrac{\mathrm{d}N_x}{\mathrm{d}x} = F^P_{x_0} \\ R\dfrac{\mathrm{d}M_x}{\mathrm{d}x} - RQ_x = F^P_{x_1} \\ R\dfrac{\mathrm{d}P_x}{\mathrm{d}x} - 2RM_{xz} = F^P_{x_2} \\ R\dfrac{\mathrm{d}S_x}{\mathrm{d}x} - 3RP_{xz} = F^P_{x_3} \\ R\dfrac{\mathrm{d}Q_x}{\mathrm{d}x} - N_\theta = F^P_{z_0} \\ R\dfrac{\mathrm{d}M_{xz}}{\mathrm{d}x} - M_\theta - RN_z = F^P_{z_1} \\ R\dfrac{\mathrm{d}P_{xz}}{\mathrm{d}x} - P_\theta - 2RM_z = F^P_{z_2} \\ R\dfrac{\mathrm{d}S_{xz}}{\mathrm{d}x} - S_\theta - 3RP_z = F^P_{z_3} \end{cases} \tag{24}$$

where F^P stand for non-homogeneity of the governing equations which have been resulted from the loading of pressure. The subscript x and z in the right terms of each equation show the component of F^P along the axial and radial direction, respectively. We have:

$$\begin{cases} F^P_{x_i} = 0 \\ F^P_{z_i} = -Rf_{sf}z^i\left(1+\dfrac{z}{R}\right)\Big|_{z=\pm\frac{h}{2}} \end{cases} \qquad i = 0,1,2,3 \tag{25}$$

and the boundary conditions at two ends of the cylinder are

$$R\big[N_x\delta u_0 + M_x\delta u_1 + P_x\delta u_2 + S_x\delta u_3 + Q_x\delta w_0 + M_{xz}\delta w_1 + P_{xz}\delta w_2 + S_{xz}\delta w_3\big]_0^L = 0 \tag{26}$$

Eqs. (24) express the main governing equations based on the TSDT for the cylindrical shells under internal or external pressure. Eq. (26) is the boundary conditions which should be satisfied at two end of the cylinder.

3 ANALYTICAL SOLUTION

In fact, Eqs. (24) are the set of differential equations. In order to solve the set of Eqs. (24), forces and moments should be written by the usage of Eqs. (11) to (18) in the terms of stresses. The stresses could be written in the terms of strains by using Eq. (7). By the usage of Eqs. (4), the strains are converted into the displacement filed components. Finally, a set of linear non-homogenous differential equations with constant coefficients would result, as follows:

$$\left[A\right]\frac{\mathrm{d}^2}{\mathrm{d}x^2}\left\{y\right\}+\left[B\right]\frac{\mathrm{d}}{\mathrm{d}x}\left\{y\right\}+\left[C\right]\left\{y\right\}=\left\{F\right\} \tag{27}$$

where $\left[A\right]_{8\times8}$, $\left[B\right]_{8\times8}$ and $\left[C\right]_{8\times8}$ are the coefficient matrices and $\left\{F\right\}$ is the force vector, which can be expressed as the set of non-homogeneity of differential equations'. $\left\{y\right\}$ is the unknown vector including the components of displacement field as:

$$\left\{y\right\}=\left\{u_0 \quad u_1 \quad u_2 \quad u_3 \quad w_0 \quad w_1 \quad w_2 \quad w_3\right\}^T \tag{28}$$

Matrix $\left[C\right]$ in the Eq. (27) which reverse would be needed in the next calculations is singular. In order to make $\left[C\right]^{-1}$, the first equation in the set of Eqs. (24) has been integrated.

$$RN_x = C_0 \tag{29}$$

In Eqs. (24), it is apparent that u_0 does not exist, but $\mathrm{d}u_0/\mathrm{d}x$ does. In order to calculate displacements in Eqs. (4), $\mathrm{d}u_0/\mathrm{d}x$ is needed. Therefore, by assuming $\mathrm{d}u_0/\mathrm{d}x=\nu$ as a new parameter which could be indicated in the following terms:

$$u_0 = \int v\,\mathrm{d}x + C_{15} \tag{30}$$

Applying the mentioned changes, the unknown vector $\left\{y\right\}$ in the set of differential Eqs. (27) would be rewritten as follows:

$$\left\{y\right\}=\left\{v \quad u_1 \quad u_2 \quad u_3 \quad w_0 \quad w_1 \quad w_2 \quad w_3\right\}^T \tag{31}$$

Non-homogeneity of the differential Eqs. (27) would be derived as follows:

$$\left\{F\right\}=\begin{Bmatrix} F_{x_0}+C_0 \\ F_{x_1} \\ F_{x_2} \\ F_{x_3} \\ F_{z_0} \\ F_{z_1} \\ F_{z_2} \\ F_{z_3} \end{Bmatrix} \tag{32}$$

The corresponding coefficient matrices $\left[A\right]$, $\left[B\right]$ and $\left[C\right]$ of the new differential Eqs. (27) have been defined in appendices.

The solution of Eqs. (27) consists of general and particular parts:

$$\{y\} = \{y\}_g + \{y\}_p \tag{33}$$

For the general solution, $\{y\}_g = \{V\}e^{mx}$ is substituted in homogeneous Eq. (27).

$$e^{mx}\left[m^2[A] + m[B] + [C]\right]\{V\} = \{0\} \tag{34}$$

Considering that e^{mx} is not equal to zero, the following determinant which is equal to zero would result.

$$\left|m^2[A] + m[B] + [C]\right| = 0 \tag{35}$$

The above determinant is a sixteen-order polynomial which is a function of m. The determinant's roots are the eigenvalues m_i consisting of eight pairs of conjugated roots where a pair of the roots is zero. Substituting the calculated eigenvalues in Eq. (34), the corresponding eigenvectors $\{V\}_i$ are obtained. Therefore, the general solution has been obtained.

$$\{y\}_g = \sum_{i=1}^{14} C_i \{V\}_i e^{m_i x} \tag{36}$$

Given that $\{F\}$ in Eq. (27) consists of constant parameters, the non-homogenous part of the solution for axisymmetric cylinder with constant thickness under uniform pressure is not the function of x. Therefore, the particular solution can be expressed as follows.

$$[C]\{y\}_p = \{F\} \Rightarrow \{y\}_p = [C]^{-1}\{F\} \tag{37}$$

Considering Eq. (26), clamped-clamped boundary conditions at two ends of the cylinder are as follows:

$$\begin{cases} x = 0 & \Rightarrow u_0 = u_1 = u_2 = u_3 = w_0 = w_1 = w_2 = w_3 = 0 \\ x = L & \Rightarrow u_0 = u_1 = u_2 = u_3 = w_0 = w_1 = w_2 = w_3 = 0 \end{cases} \tag{38}$$

Applying eight boundary conditions at each end of the cylinder, sixteen constants comprised of $C_1,\ldots,C_{14}$ in the general solution and C_0, C_{15} in the particular solution would be calculated. Finally, the unknown vector $\{y\}$ which consists of displacement field components would be obtained in terms of x variable based on Eq. (33) by determining unknown constants. Using Eq. (3) would result radial and axial displacements. Stress distribution would be obtained by using Eqs. (4) and (7).

4 RESULTS AND DISCUSSIONS

As a case study, we consider a thick cylinder whose elasticity modulus varies in radial direction and has the following characteristics: $r_i = 40$ mm, $h = 20$ mm and $L = 0.8$ m. The elasticity modulus at the internal radius and Poisson's ratio have values of $E_i = 200$ GPa and $\nu = 0.3$, respectively. The applied internal and external pressures are $P_i = P_0 = 80$ MPa. The analytical solution is carried out by writing the program in MAPLE 17.

In order to show the abilities of the presented analytical solution for analyzing a FG cylinder, a numerical solution has been investigated. The ANSYS 14.5 package was used in the static analysis of thick hollow cylinder with constant thickness. The PLANE82 element in axisymmetric mode, which is an element with eight nodes and two translational degrees of freedom in the axial and radial directions per each node, was used for modeling. In order to consider the radial continuous varying of elastic modulus along the thickness of cylindrical shell with an exponential function, the thickness of cylinder has been divided to some homogeneous layers. Each layer's properties have been defined as an exponential function of the distance of layer's middle from internal layer. Finally the cylindrical shell consists of some coherent homogeneous layers whose properties at the contact location of the layers are the average of left and right limit of two layers' boundaries. Dividing the thickness of the cylinder into 40 layers causes the results of numerical modeling to converge to the results of analytical solution. Internal and external pressures are applied to the nodes of inner and outer layers, respectively. Clamped boundary conditions have been exerted by preventing the nodes around two ends of the cylinder from movement.

In the next sections, the effect of internal and external pressure on FG cylinder has been investigated for clamped-clamped boundary conditions. Considering the fact that behavior of the cylinder subjected to the effect of internal and external pressure are similar, most of the graphs are depicted along the radial direction at the middle of the cylinder in the section of internal pressure effect while the displacements and stresses have been investigated along the longitudinal direction of the cylinder in the section of external one.

4.1 Internal pressure effect

Figure 2 shows the distribution of the dimensionless radial displacement resulted from the numerical and analytical solution at middle of a cylinder under internal pressure. It is seen that for negative values of n, the displacements of FGM cylinders are higher than of a homogeneous cylinder. For positive values of n, the situation is reverse, i.e. the displacement is lower. The variation in the displacement of heterogeneous material is similar to that of homogenous material. Furthermore, the maximum values of radial displacements are observed in internal surface.

Figures 3 and 4 show the distribution of the dimensionless circumferential and effective stress resulting from the numerical and analytical solution at $x = L/2$ of cylinder under internal pressure, respectively. It is obviously observed that both stresses along the thickness of the cylinder show the same behavior while the effective stresses have higher values. The both stresses for negative values of n are higher than the homogenous materials at layers close to the internal surface while at the outer surface, it is less than the homogenous materials. For positive values of n, the reverse holds true, suggesting that the heterogonous materials have less values of stress than the homogenous ones at inner surfaces and the higher values of stress at outer surfaces. Considering more uniform

stress distribution of the layers and less maximum values of stress for $n < 0$ under combined loading, it is interesting to use FG materials with positive values of n for cylinder under internal pressure.

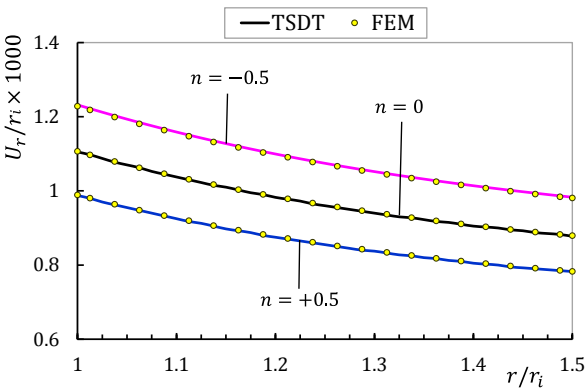

Figure 2: Dimensionless radial displacement at $x = L/2$ under internal pressure.

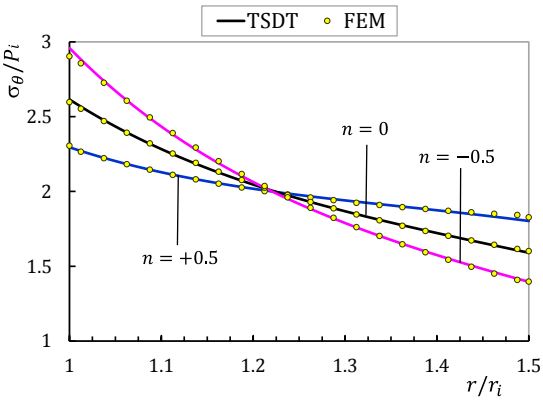

Figure 3: Dimensionless circumferential stress at $x = L/2$ under internal pressure.

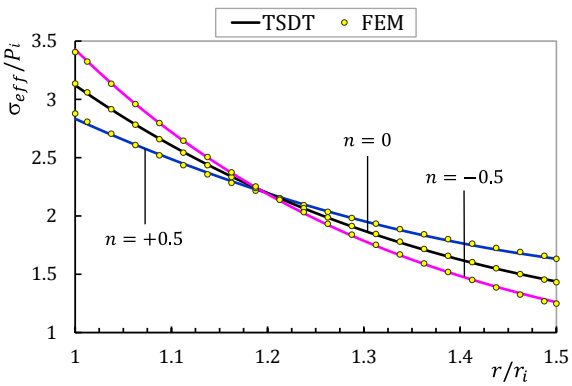

Figure 4: Dimensionless effective stress at $x = L/2$ under internal pressure.

Dimensionless effective stress distribution under combined load at $z = 0$ along the longitudinal direction of the cylinder for different materials are illustrated in Figure 5. It could be observed that effective stress along the longitudinal direction is uniform except the layers around the clamped boundaries. Therefore, PET results are valid through the length of the cylinder far away from clamped boundaries. The higher values of effective stress for positive inhomogeneity at middle surface of the cylinder (Figure 5) show the fact that the point around which the effective stress graphs meet each other in Figure 4 is close to the internal half of the cylinder under internal pressure. Figure 5 shows that effective stresses at middle layer of the cylinder under internal pressure for positive inhomogeneity constants are higher that the negative one at all points of the longitudinal direction, even at peak around clamped ends. Considering this fact reveal that the trend of effective stress of any layer along the thickness retain constant along longitudinal direction, i.e. the effective stress of FGM cylinder at internal layer (critical layer) for $n < 0$ is higher than $n > 0$ and this trend appear at all points of the internal layer along longitudinal direction. Therefore, the results at middle of the cylinder $\left(x = L/2\right)$ are valid for conclusion about the suitable FGM inhomogeneity constant.

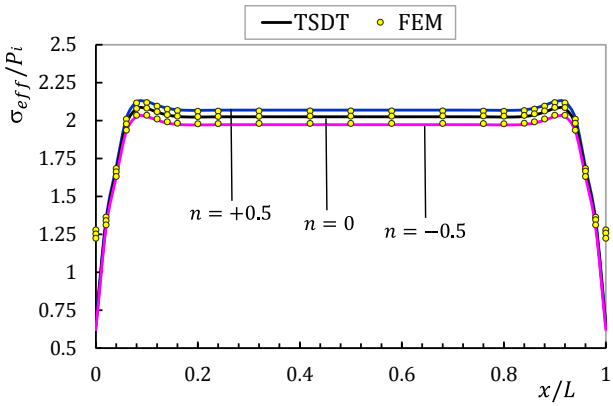

Figure 5: Dimensionless effective stress at $z = 0$ under internal pressure.

4.2 External pressure effect

Figures 6 and 7 show the distribution of the dimensionless radial and axial displacement along the longitudinal direction in the middle surface of the cylinder under external pressure for different inhomogeneity constants. The external pressure, as the internal one, causes less values of displacements for positive inhomogeneity constants in FGM cylinder. Therefore, usage of cylinder made up of positive inhomogeneity constants is more suitable from the view point of lower displacement. The responses of an FG cylinder under mechanical loads can be considered in order to evaluate the effect of inhomogeneity of used materials. Furthermore, the effect of end condition of the cylinder can be considered on the longitudinal distribution of the responses. This consideration can determine the longitudinal range of effect of the supports on the responses.

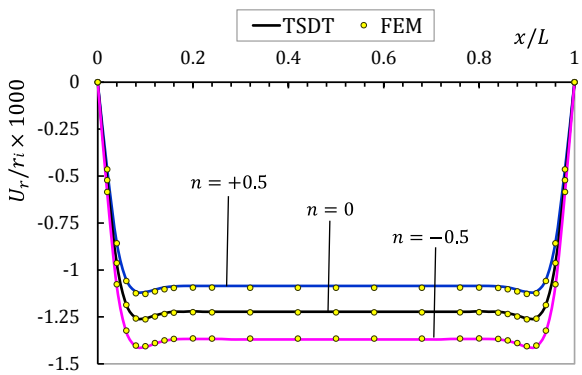

Figure 6: Dimensionless radial displacement at $z = 0$ under external pressure.

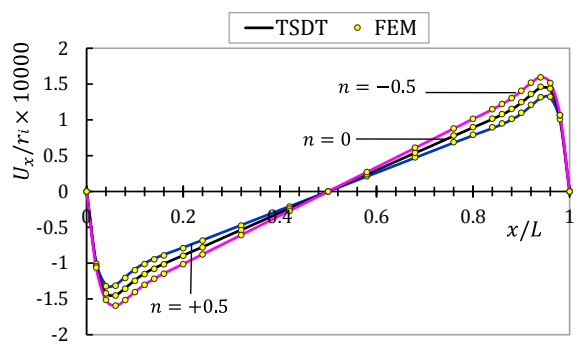

Figure 7: Dimensionless longitudinal displacement at $z = 0$ under external pressure.

Figures 8 and 9 show the circumferential stress along the longitude and thickness of the cylinder under external pressure, respectively. Comparison of Figures 3, 8 and 9 show that the circumferential stress of the cylinder under internal or external pressure are similar, means that the higher values of stresses are observed in materials with negative inhomogeneity constants. However, external pressure causes higher and negative circumferential stresses in comparison with the internal pressure of the same value. As the terms resulting from pressure have been revealed in the non-

homogeneity part of the set of governing differential equations, the superposition principle could be utilized for the effect of combined loading on the basis of linear elasticity. In fact, the non-homogeneity vector $\{F\}$ appears as a force vector in the governing equations. Therefore, under the effect of combined loading including internal and external pressure with the same value, the effect of external pressure is dominant means that the circumferential stress would be negative. Furthermore, the higher values of circumferential stress for positive inhomogeneity at middle surface of the cylinder under external pressure (Figure 8) show the same results for the position of the point around which the effective stress graphs meet each other (Figure 9).

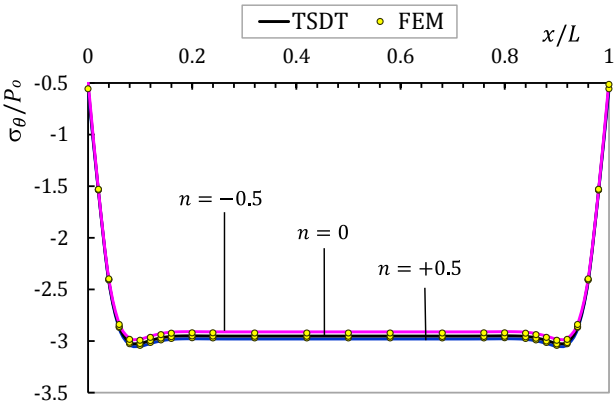

Figure 8: Dimensionless circumferential stress at $z = 0$ under external pressure.

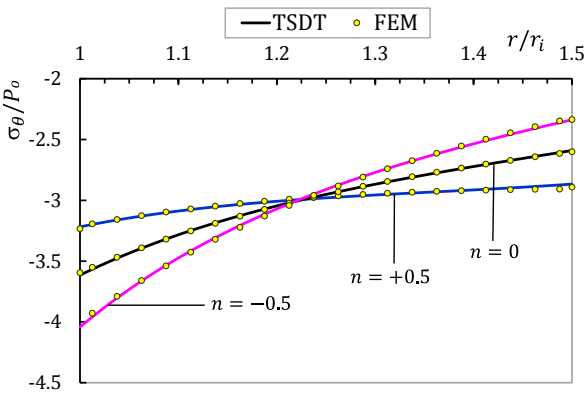

Figure 9: Dimensionless circumferential stress at $x = L/2$ under external pressure.

Distribution of dimensionless longitudinal and effective stress in middle layer of cylinder are shown in Figures 10 and 11. At points away from the boundaries, axial stress does not show considerable differences in cylinder made up of different FG materials unlike the circumferential and effective stress, while at points near the boundaries, the reverse holds true. Comparison of Figures 5 and 11 show higher values of effective stresses resulted from external pressure to the internal one. Figure 10 show that the axial stress distribution (unlike circumferential and effective one) have not constant trend along the longitudinal direction, i.e. the axial stress of FG cylinder with negative inhomogeneity constant is higher than the positive one far away from boundaries while at peak points near two ends, reverse hold true means that positive constants cause higher axial stress. Therefore, the results of axial stress (unlike circumferential and effective one) at middle of the cylinder are not valid for selecting appropriate FG material.

4.3 Higher-order approximation effect

Tables 1, 2 and 3 present the radial displacement, circumferential and effective stresses of different layers resulting from SDT and FEM in the middle of heterogeneous cylinder ($x = L/2$) under internal pressure, respectively. The FSDT solution procedure has been explained in the references (Ghannad and Zamani Nejad, 2010). It is observed that FSDT has acceptable results in middle layer while the results of the other layers (especially stress results) show a significant difference once compared with the results calculated from TSDT and FEM solution.

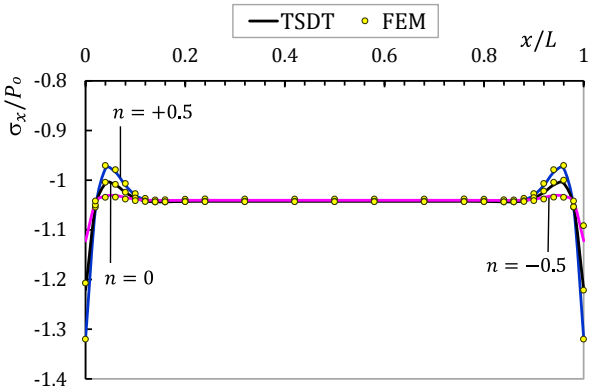

Figure 10: Dimensionless longitudinal stress at $z = 0$ under external pressure.

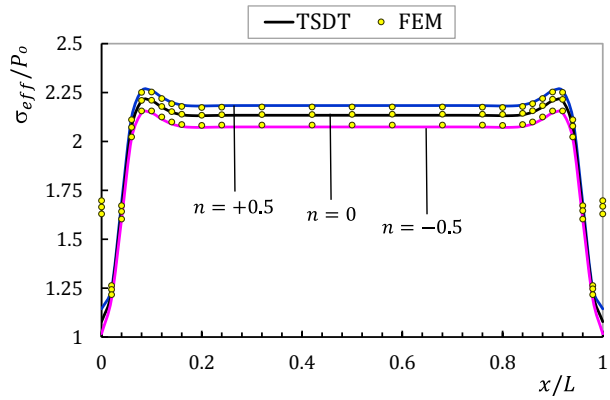

Figure 11: Dimensionless effective stress at $z = 0$ under external pressure.

U_r (mm)	$n = -0.5$			$n = 0$			$n = +0.5$		
	TSDT	FSDT	FEM	TSDT	FSDT	FEM	TSDT	FSDT	FEM
internal layer	0.04927	0.04732	0.04912	0.04420	0.04250	0.04425	0.03950	0.03800	0.03955
middle layer	0.04297	0.04256	0.04286	0.03840	0.03830	0.03845	0.03421	0.03421	0.03424
external layer	0.03931	0.03780	0.03921	0.03510	0.03400	0.03516	0.03130	0.03041	0.03129

Table 1: The results of radial displacement at the middle of the cylinder under internal pressure.

σ_θ (MPa)	$n = -0.5$			$n = 0$			$n = +0.5$		
	TSDT	FSDT	FEM	TSDT	FSDT	FEM	TSDT	FSDT	FEM
internal layer	236.697	262.224	232.280	209.190	235.785	207.740	183.621	210.928	184.460
middle layer	153.333	152.576	154.020	156.114	155.618	156.190	158.120	157.909	158.000
external layer	111.703	88.266	111.760	127.246	102.174	128.120	144.212	117.666	146.140

Table 2: The results of circumferential stress at the middle of the cylinder under internal pressure.

σ_{eff} (MPa)	$n = -0.5$			$n = 0$			$n = +0.5$		
	TSDT	FSDT	FEM	TSDT	FSDT	FEM	TSDT	FSDT	FEM
internal layer	274.316	228.089	272.440	249.672	204.728	250.900	226.676	182.822	230.170
middle layer	157.824	158.394	158.000	161.984	161.098	162.040	165.504	163.011	165.010
external layer	100.802	115.261	99.786	115.001	132.828	114.310	130.597	152.293	130.470

Table 3: The results of effective stress at the middle of the cylinder under internal pressure.

It is generally observed that higher order approximation of displacement field components in comparison with FSDT yields error reduction. The reason is that FSDT assumes linear distribution for the radial displacement while according to the lame's theory (PET), the variation of radial displacement along the thickness of the cylinder has hyperbolic distribution (Ghannad and Zamani Nejad, 2012).

$$U_r(r) = C_1 r + \frac{C_2}{r} \tag{39}$$

Therefore, the linear distribution is not appropriate approximation except the middle layer where the parameter z is equal to zero. Because of indirect stress calculations, the incoherence of results intensifies for stresses in compared with displacements.

Effective stresses resulted from TSDT, PET and FEM at middle layer of cylinder and $x = L/2$ under internal and/or external pressure are shown in Table 4. The PET solution is carried out for cylinder under plane strain condition.

σ_{eff} (MPa)	$n = -0.5$			$n = 0$			$n = +0.5$		
	TSDT	PET	FEM	TSDT	PET	FEM	TSDT	PET	FEM
$P_i = 80\,\text{MPa}$	157.82	158.01	158.00	161.98	161.67	162.04	165.50	164.62	165.01
$P_0 = 80\,\text{MPa}$	165.91	165.55	166.68	170.69	169.70	171.04	174.66	172.98	174.04
$P_i = P_0 = 80\,\text{MPa}$	32.79	32.06	32.06	32.82	32.00	32.02	32.74	31.90	31.92

Table 4: The results of effective stress at the middle of the cylinder for different loading.

5 CONCLUSIONS

In this paper, an analytical solution based on TSDT and FEM is conducted for axisymmetric thick FG pressurized cylinders under clamped ends condition, and has been compared with results of homogenous cylinders. The variation of FGM properties is supposed to be an exponential function along the thickness of cylinders. The analytical solutions and the solutions carried out through the FEM show good agreement. Furthermore, the effect of higher order approximation and internal/external pressure has been conducted. It is observed that usage of cylinder made up of positive inhomogeneity constants is more suitable from the view point of lower displacement. The results show that from the view point of uniform stress distribution of the layers and less maximum values of stress for $n < 0$ under combined loading, it is interesting to use FG materials with positive values of n for pressurized cylinder. At points away from the boundaries, axial stress does not show considerable differences in cylinder made up of different FG materials unlike the circumferential and effective stress, while at points near the boundaries, the reverse holds true. The results show higher values of stresses resulted from external pressure to the internal one. As the terms resulting from pressure have been revealed in the non-homogeneity part of the set of governing differential equations, the superposition principle could be utilized for the effect of combined loading on the basis of linear elasticity. Therefore, under the effect of combined loading including internal and external pressure with the same value, the effect of external pressure is dominant which yield to negative circumferential stress. Comparison between the FSDT and TSDT indicates that the maximum difference between these theories is about 4% at radial displacement and 24% at effective stress which are appeared at the internal layer. This difference implies that the assumption of linear distribution for displacement fields in FSDT is not accurate especially in stress calculus and the higher-order approximation is needed. Although TSDT method has acceptable results for displacements and

circumferential and axial stresses, the radial and consequently von Mises stresses resulted from TSDT show slight difference by the results calculated from PET solution. The maximum difference between the effective stress resulted from PET and TSDT at middle layer of cylinder under internal and/or external pressure is less than 1%. This difference increase at layers close to the boundaries and the greatest difference occurs in the internal surface $\left(z = -h/2\right)$. Therefore, effective stresses calculated by FEM have more coincidence by PET results than SDT.

References

Eipakchi, H.R., Rahimi, G.H., Khadem, S.E., (2003). Closed form solution for displacements of thick cylinders with varying thickness subjected to nonuniform internal pressure. J. Structural Engineering and Mechanics 16(6): 731-748.

Eipakchi, H.R., Khadem, S.E., Rahimi, G.H., (2008). Axisymmetric stress analysis of a thick conical shell with varying thickness under nonuniform internal pressure. J. Engineering Mechanics 134: 601-610.

Eipakchi, H.R., (2010). Third-order shear deformation theory for stress analysis of a thick conical shell under pressure. J. of Mechanics of materials and structures 5(1): 1-17.

Fukui, Y., Yamanaka, N., (1992). Elastic analysis for thick-walled tubes of functionally graded materials subjected to internal pressure. JSME, Ser. I 35(4): 891-900.

Ghannad, M., Zamani Nejad, M., (2010). Elastic analysis of pressurized thick hollow cylindrical shells with clamped-clamped ends. Mechanika 5(85): 11-18.

Ghannad, M., Zamani Nejad, M., (2012). Complete elastic solution of pressurized thick cylindrical shells made of heterogeneous functionally graded materials. Mechanika 18(6): 640-649.

Ghannad, M., Rahimi, G.H., Zamani Nejad, M., (2013). Elastic analysis of pressurized thick cylindrical shells with variable thickness made of functionally graded materials. Composites: Part B 45: 388-396.

Greenspon, J.E., (1960). Vibration of a thick-walled cylindrical shell, comparison of the exact theory with approximate theories. J. of the Acoustical Society of America 32(5): 571-578.

Hongjun, X., Zhifei, S., Taotao, Z., (2006). Elastic analyses of heterogeneous hollow cylinders. J. of Mechanics, Research Communications 33(5): 681-691.

Kumar, A., Chakrabarti, A., Ketkar, M., (2013). Analysis of laminated composite skew shells using higher order shear deformation theory. Latin American j. of solids and structures 10(5): 919-931.

Mirsky, I., Hermann, G., (1958). Axially motions of thick cylindrical shells. J. of Applied Mechanics-Transactions of the ASME 25: 97-102.

Reddy, J.N., Liu, C.F., (1985). A higher-order shear deformation theory of laminated elastic shells. International J. of Engineering Science 23: 319–330.

Simkins, T.E., (1994). Amplifications of flexural waves in gun tubes. J. of Sound and Vibration 172(2): 145-154.

Tutuncu, N., (2007). Stresses in thick-walled FGM cylinders with exponentially-varying properties. J. Engineering Structures 29: 2032-2035.

Tutuncu, N., Temel, B., (2009). A novel approach to stress analysis of pressurized FGM cylinders, disks and spheres. Composite Structures 91: 385-390.

Zamani Nejad, M., Rahimi, G.H., Ghannad, M., (2009). Set of field equations for thick shell of revolution made of functionally graded materials in curvilinear coordinate system. Mechanika 3(77): 18-26.

Zhifei, S., Taotao, Z., Hongjun, X., (2007). Exact solutions of heterogeneous elastic hollow cylinders. Composite Structures 79(1): 140-147.

APPENDICES

$$\left[A\right]=\begin{bmatrix}\left[A_{11}\right]_{4*4} & \left[A_{12}\right]_{4*4}\\ \left[A_{21}\right]_{4*4} & \left[A_{22}\right]_{4*4}\end{bmatrix} \tag{A1}$$

$$\left[A_{12}\right]=\left[A_{21}\right]=0 \tag{A2}$$

$$\left[A_{11}\right]_{ij}=\begin{cases}R\lambda'\int\limits_{-h/2}^{h/2}e^{n\left(\overline{r}-1\right)}\left(1-\nu\right)\left(1+\dfrac{z}{R}\right)z^{\left(i+j-2\right)}\,\mathrm{d}z & i,j=2,3,4\\ 0 & \text{else}\end{cases} \tag{A3}$$

$$\left[A_{22}\right]_{ij}=\begin{cases}R\lambda'\int\limits_{-h/2}^{h/2}ke^{n\left(\overline{r}-1\right)}\left(1-\nu\right)\left(1+\dfrac{z}{R}\right)z^{\left(i+j-2\right)}\,\mathrm{d}z & i,j=1,2,3,4\end{cases} \tag{A4}$$

$$\left[B\right]=\begin{bmatrix}\left[B_{11}\right]_{4*4} & \left[B_{12}\right]_{4*4}\\ \left[B_{21}\right]_{4*4} & \left[B_{22}\right]_{4*4}\end{bmatrix} \tag{A5}$$

$$\left[B_{22}\right]=0 \tag{A6}$$

$$\left[B_{21}\right]=-\left[B_{12}\right]^{T} \tag{A7}$$

$$\left[B_{11}\right]_{ij}=\begin{cases}R\lambda'\int\limits_{-h/2}^{h/2}e^{n\left(\overline{r}-1\right)}\left(1-\nu\right)\left(1+\dfrac{z}{R}\right)z^{\left(i+j-2\right)}\,\mathrm{d}z & \begin{matrix}i=1,\ j=2,3,4\\ j=1,\ i=2,3,4\end{matrix}\\ 0 & \text{else}\end{cases} \tag{A8}$$

$$\left[B_{12}\right]_{ij}=\begin{cases}0 & i\ =1\\ \lambda'\int\limits_{-h/2}^{h/2}e^{n\left(\overline{r}\right)-1}\left\{z\left[j\nu-\left(i-1\right)k\right]+\left[R\left(\left(j-1\right)\nu-\left(i-1\right)k\right)\right]\right\}z^{\left(i+j-3\right)}\,\mathrm{d}z & \text{else}\end{cases} \tag{A9}$$

$$\left[C\right]=\begin{bmatrix}\left[C_{11}\right]_{4*4} & \left[C_{12}\right]_{4*4}\\ \left[C_{21}\right]_{4*4} & \left[C_{22}\right]_{4*4}\end{bmatrix} \tag{A10}$$

$$\left[C_{21}\right]=-\left[C_{12}\right]^{T} \tag{A11}$$

$$\left[C_{11}\right]_{ij}=\begin{cases}R\lambda'\int\limits_{-h/2}^{h/2}e^{n\left(\overline{r}-1\right)}\left(1-\nu\right)\left(1+\dfrac{z}{R}\right)\mathrm{d}z & i,j=1\\ -\left(i-1\right)\left(j-1\right)R\lambda' k\int\limits_{-h/2}^{h/2}e^{n\left(\overline{r}-1\right)}\left(1+\dfrac{z}{R}\right)z^{\left(i+j-4\right)}\,\mathrm{d}z & \text{else}\end{cases} \tag{A12}$$

$$\left[C_{12}\right]_{ij} = \begin{cases} \lambda' \int_{-h/2}^{h/2} \nu e^{n\left(\overline{r}-1\right)} \,\mathrm{d}z & i,j=1 \\ \lambda' \int_{-h/2}^{h/2} \nu e^{n\left(\overline{r}-1\right)} z^{j-2}\left[\left(j-1\right)R + jz\right] \mathrm{d}z & i=1, j=2,3,4 \\ 0 & \text{else} \end{cases} \tag{A13}$$

$$\left[C_{22}\right]_{ij} = \begin{cases} -\lambda' \int_{-h/2}^{h/2} e^{n\left(\overline{r}-1\right)} \left[\left(\left(i-1\right)\left(j-1\right)\left(R+z\right)\left(1-\nu\right)\right) + \left(\left(i+j-2\right)\nu\right)z + \left(\frac{1-\nu}{R+z}\right)z^2\right] z^{\left(i+j-4\right)} \,\mathrm{d}z \\ i\ ,\ \ j=1,2,3,4 \end{cases} \tag{A14}$$

where the parameters λ' and k are as follows

$$\lambda' = \frac{E_i}{\left(1+\nu\right)\left(1-2\nu\right)} \tag{A15}$$

$$k = \left(\frac{1-2\nu}{2}\right) \tag{A16}$$